Journal of Solid State Chemistry 187 (2012) 1–6

Contents lists available at SciVerse ScienceDirect

Journal of Solid State Chemistry

journal homepage: www.elsevier.com/locate/jssc

New $CeMgCo_4$ and Ce_2MgCo_9 compounds: Hydrogenation properties and crystal structure of hydrides

R.V. Denys [a], A.B. Riabov [a,*], R. Černý [b], I.V. Koval'chuk [a], I.Yu. Zavaliy [a]

[a] Karpenko Physico-Mechanical Institute NAS Ukraine, 5, Naukova Street, Lviv, 79000, Ukraine
[b] Laboratory of Crystallography, University of Geneva, 24, Quai Ansermet, Geneva, Switzerland

ARTICLE INFO

Article history:
Received 22 August 2011
Received in revised form
19 October 2011
Accepted 24 October 2011
Available online 7 November 2011

Keywords:
Hydrogen storage
Metal hydride
Magnesium compounds
Pressure–Composition–Temperature relationships
Neutron diffraction

ABSTRACT

Two new ternary intermetallic compounds, $CeMgCo_4$ (C15*b* pseudo-Laves phase, $MgCu_4Sn$ type) and Ce_2MgCo_9 (substitution derivative of $PuNi_3$ type) were synthesized by mechanical alloying method. The structural and hydrogenation properties of these compounds were studied by X-ray diffraction and Pressure–Composition–Temperature measurements. Both compounds absorb hydrogen at room temperature and pressures below 10 MPa forming hydrides with maximum compositions $CeMgCo_4H_6$ and $Ce_2MgCo_9H_{12}$. Single plateau behavior was observed in *P–C* isotherm during hydrogen absorption/desorption by Ce_2MgCo_9 alloy. The $CeMgCo_4$–H_2 system is characterized by the presence of two absorption/desorption plateaus corresponding to formation of β-$CeMgCo_4H_4$ and γ-$CeMgCo_4H_6$ hydride phases. The structure of β-hydride $CeMgCo_4H(D)_4$ was determined from X-ray and neutron powder diffraction data. In this structure initial cubic symmetry of $CeMgCo_4$ is preserved and hydrogen atoms fill only one type of interstitial sites, triangular $MgCo_2$ faces. These positions are occupied by 70% and form octahedron around Mg atom with Mg–D bond distances 1.84 Å.

1. Introduction

In recent years substantial efforts of researchers have been focused on the implementation of magnesium and its compounds into hydrogen storage technologies. There are two principal directions of such researches. The first one is the creation of nanoscale magnesium-based composites, which are capable of absorbing and desorbing hydrogen at substantially lower temperatures than pure magnesium metal [1,2]. Another direction is the development of new ternary or pseudo-binary Mg-containing compounds, able to absorb H_2 reversibly at ambient conditions. Among such compounds one should mention recently studied Mg_3TNi_2 (*T*=Ti, Al, Mn) derivatives of Ti_2Ni-type [3,4] and hybrid $(La_{1-x}Mg_x)_nNi_m$ compounds [5–7]. Important part of this group are cubic *RE*$MgNi_4$ compounds ($MgCu_4Sn$ type), which can be considered as derivatives of cubic $AuBe_5$ type of structure, in which Au and one of positions of Be are substituted by rare-earth and magnesium atoms, respectively. These compounds of the $MgCu_4Sn$ type are often considered as ordered derivative of C15 cubic Laves phase, in which half of Mg is substituted by rare earth metal and referred as C15*b* phases [8].

The last group of compounds is being studied since 1980 [9] when the first its representative, $LaMgNi_4$, had been synthesized. Later it has been shown that such compounds exist in other *RE*–Mg–Ni systems, like *RE*=Ca, Sc, Y, rare-earth metal [10–13]. Such compounds have been found to absorb hydrogen [14–17]. Structures of hydrides of $LaMgNi_4$ and $NdMgNi_4$ compounds have been determined by neutron diffraction [16]. Similar to the above mentioned Mg-containing Mg_3TNi_2 and $(La_{1-x}Mg_x)_nNi_m$ compounds [4,5], Ni-containing C15*b* pseudo-Laves phases have been shown to be suitable for electrodes in Ni–MH batteries [18]. At the same time, C15*b* pseudo-Laves phases in the Co-containing systems have not been studied so far.

The paper is focused on synthesis of Ce–Mg–Co compounds, determination of their hydrogenation properties and structure of $CeMgCo_4D_4$ deuteride.

2. Experimental part

Starting materials for preparation of Ce–Mg–Co samples were ingots of Ce and Co, and Mg powder (all with purities ≥99.9%). In the first step, $CeCo_4$ and Ce_2Co_9 alloy precursors were prepared by arc melting in argon atmosphere. The arc-melted Ce–Co alloys were then ground in a glove box and mixed with Mg powder in suitable proportions. The mixtures were ball-milled under Ar atmosphere in sealed stainless still vials using SPEX 8000D mill. The powders, obtained after 6 h of milling have been reloaded into tantalum container and annealed at 800 °C for 7 h under 1 bar Ar.

* Corresponding author.
E-mail address: alexr@ipm.lviv.ua (A.B. Riabov).

0022-4596/$ - see front matter © 2011 Elsevier Inc. All rights reserved.
doi:10.1016/j.jssc.2011.10.040

Phase analysis of the samples was carried out by X-ray powder diffraction (Fe–Kα, DRON-3.0 diffractometer). Structural characterization of alloys and hydrides was performed by high resolution synchrotron X-ray diffraction (λ=0.6513 Å) collected at the powder diffraction beamline B2 at HASYLAB/DESY (Hamburg, Germany) [19].

Hydrogen absorption–desorption properties were investigated using a Sieverts' type volumetric apparatus in the temperature range between 0 and 75 °C and pressure ranging from 0.01 to 100 bar. The sample was activated in vacuum at 300 °C for 30 min, cooled to room temperature and then charged with high purity hydrogen gas (purity 99.999%). Several complete hydrogen absorption–desorption cycles were performed prior to the Pressure–Composition–Temperature (PCT) measurements to improve the kinetics of hydrogen exchange and to achieve maximum hydrogen storage capacities.

The $CeMgCo_4$-based deuteride for neutron diffraction experiment was synthesized by deuterium gas charging of the alloy in a Sieverts'-type apparatus. Prior to the synthesis the alloy activated in vacuum at 350 °C, then deuterated under 10 bar D_2 (99.8% purity) for 1 day. The deuteride was reloaded into a vanadium can (d=6 mm), sealed with indium wire. Neutron diffraction data were collected using a high resolution powder diffractometer HRPT (λ=1.494 Å, 2θ range 4.05–164.9°, step 0.05°) [20] at the Spallation Neutron Source SINQ accommodated at Paul Scherrer Institute, Villigen, Switzerland. All diffraction data were refined using the program FullProf [21].

3. Results and discussions

3.1. Structure of Ce–Mg–Co intermetallic compounds

In the present work, the attempt to synthesize $CeMgCo_4$ intermetallic compound from stochiometric amounts of Mg and $CeCo_4$ pre-alloy (1:1) resulted in formation of two-phase alloy. In addition to target cubic $CeMgCo_4$ compound of $MgCu_4Sn$ type (space group $F\bar{4}3m$; a=7.0599(2) Å; 51(1) wt%), X-ray phase analysis revealed also formation of $PuNi_3$-type rhombohedral $Ce_{2.1(1)}Mg_{0.9(1)}Co_9$ phase (space group $R\bar{3}m$; a=4.9524(3); c=24.258(3) Å; 49(1) wt%). Apparently, the formation of the second phase is caused by loss of magnesium because of its partial evaporation during annealing procedure. This two-phase alloy has been used in further synthesis of deuteride for neutron diffraction analysis.

Both ternary phases were observed for the first time in *RE*–Mg–Co systems. For investigation of their structure and hydrogenation properties we have prepared single-phase $CeMgCo_4$ and Ce_2MgCo_9 samples. A small excess of Mg was introduced into initial mixtures to compensate for its evaporation during synthesis of these samples.

SR XRD diffraction patterns of single-phase samples are shown in Fig. 1, corresponding atomic parameters are provided in Table 1. The most distinctive superstructure peaks of the ordered $CeMgCo_4$ (space group $F\bar{4}3m$), forbidden in the C15 Laves phase (space group $Fd\bar{3}m$) are marked in Fig. 1a. These peaks appear as a result of ordering of Ce and Mg atoms between two subsets (4*a* and 4*c*) of the original 8*a* positions in $Fd\bar{3}m$ of the $MgCu_2$ type. The lattice parameter of the cubic $CeMgCo_4$ C15*b* Laves phase of 7.06182(7) Å is expectedly smaller than that of the binary $CeCo_2$ ($Fd\bar{3}m$; a=7.1606 Å [22]). These lattice dimensions are quite similar with those for the isostructural $CeMgNi_4$ compound (a=7.0373(4) Å [15] and a=7.03964(5) Å, our results).

In the structure of Ce_2MgCo_9, which is a substitution derivative of $CeCo_3$, magnesium atoms selectively partially replace Ce ones in the 6*c* position. The same type of replacement has been observed earlier in the structure of $La_{3-x}Mg_xNi_9$ compounds [7]. The Ce–to–Mg replacement is accompanied by shrinking of the unit cell by ~2% mostly in the [001] direction (compare with $CeCo_3$: a=4.955; c=24.72 Å [22]).

The refinement of the structure of $CeMgCo_4$ revealed that complete Ce/Mg ordering provides negative values of atomic displacement parameter for Ce atoms. Therefore we have assumed partial disorder of magnesium and cerium between 4*a* and 4*c* sites of the $MgCu_4Sn$-type structure. In order to fix the overall phase composition we have introduced corresponding constraint for Ce/Mg occupancies of sites. It should be noted that similar disorder is observed in the structure of $CeMgNi_4$ alloy [15]. Such exchange phenomenon has been observed mostly for materials obtained with the use of mechanical alloying, while melted ones have an ordered structure [15]. Apparently, such *RE*–Mg disordering can be removed by longer annealing at higher temperature.

Attempt to synthesize similar ternaries in the La–Mg–Co system yielded mixtures of binary compounds: $LaCo_{13}$ ($NaZn_{13}$ type; $Fm\bar{3}c$; a=11.343 Å), $LaMg_3$ (BiF_3 type;$Fm\bar{3}m$; a=7.508 Å)

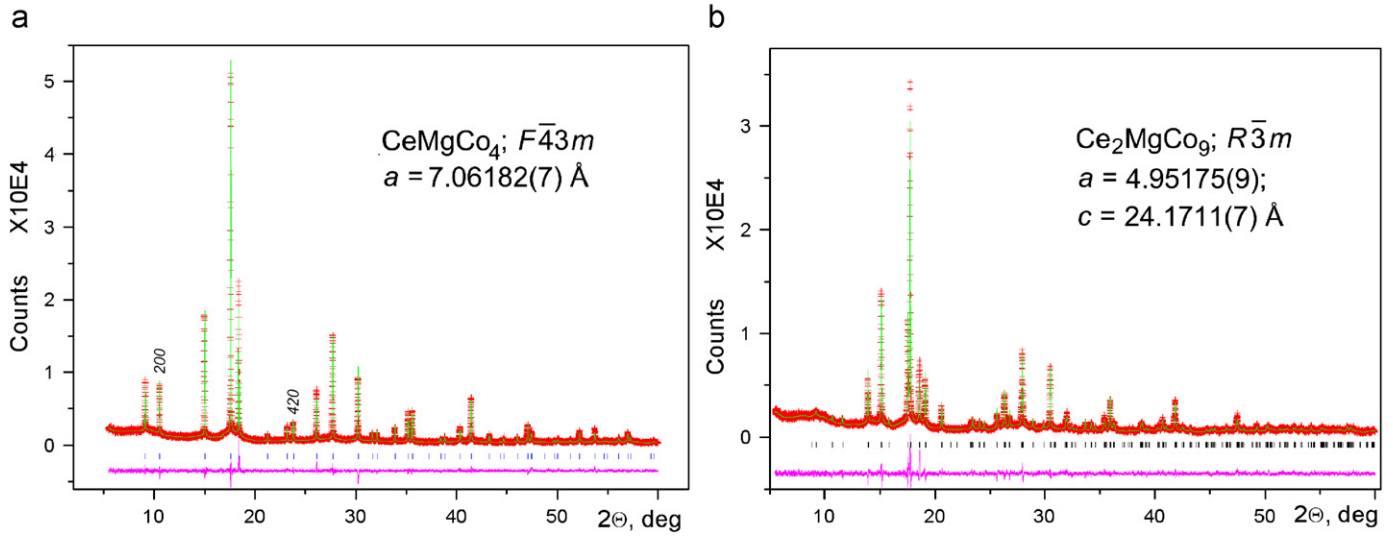

Fig. 1. SR XRD patterns (λ=0.6513 Å) of $CeMgCo_4$ (*a*, R_p=8.40; R_{wp}=11.1; R_B=6.31) and Ce_2MgCo_9 (*b*, R_p=8.31; R_{wp}=10.7; R_B=8.17). In the upper figure peaks distinguishing patterns of C15*b* structure from that of the C15 one are marked by the Miller indices.

Table 1
Atomic parameters of $CeMgCo_4$ and Ce_2MgCo_9 as-annealed alloys.

Experiment		Fe–Kα (λ=1.9361 Å)					SR XRD (λ=0.6513 Å)				
Atom	Site	x	y	z	U_{ISO}, $\times 10^2$ Å^2	S.O.F.	x	y	z	U_{ISO}, $\times 10^2$ Å^2	S.O.F.
$CeMgCo_4$		a=7.0599(2) Å; V=351.89(2) Å^3					a=7.06182(7) Å; V=352.17(1) Å^3				
Ce1	4*a*	0	0	0	0.4(2)	0.94(1)	0	0	0	0.49(1)	0.901(2)
Mg1						0.06(1)					0.099(2)
Mg2	4*c*	1/4	1/4	1/4	2.2(8)	0.94(1)	1/4	1/4	1/4	2.0(1)	0.901(2)
Ce2						0.06(1)					0.099(2)
Co	16*e*	0.6235(5)	x	x	0.5(1)	1.0(–)	0.6240(1)	x	x	0.58(2)	1.0(–)
Ce_2MgCo_9		$Ce_{2.1}Mg_{1.9}Co_9$ a=4.9524(3); c=24.258(3) Å; V=515.2(1) Å^3					$Ce_{1.96}Mg_{1.04}Co_9$ a=4.95175(9); c=24.1711(7) Å; V=513.27(3) Å^3				
Ce1	3*a*	0	0	0	1.0(–)	1.0(–)	0	0	0	0.63(3)	1.0(0)
Ce2	6*c*	0	0	0.1405(7)	1.5(–)	0.55(3)	0	0	0.1422(1)	1.48(3)	0.479(5)
Mg2						0.45(3)					0.521(5)
Co1	3*b*	0	0	1/2	0.5(–)	1.0(–)	0	0	1/2	0.58(7)	1.0(–)
Co2	6*c*	0	0	0.3341(9)	0.5(–)	1.0(–)	0	0	0.3342(2)	0.11(3)	1.0(–)
Co5	18*g*	0.498(2)	$-x$	0.0838(6)	0.5(–)	1.0(–)	0.5015(3)	$-x$	0.08332(8)	0.55(3)	1.0(–)

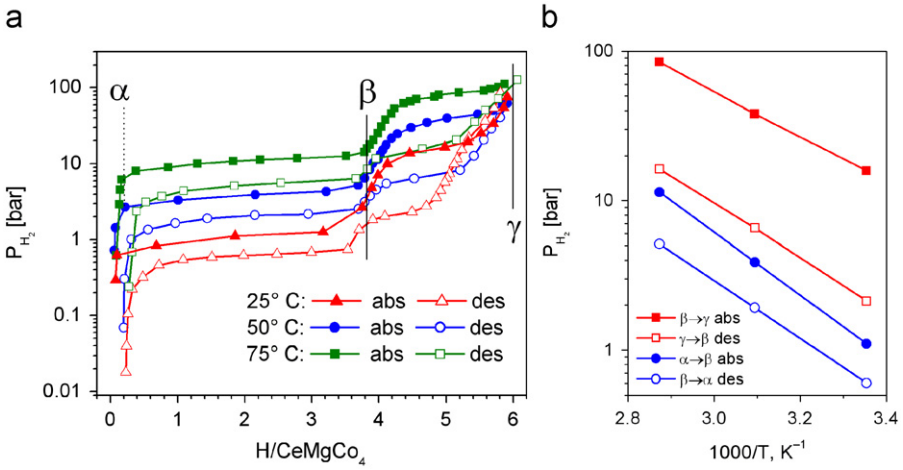

Fig. 2. PCT dependences for the $CeMgCo_4$–H_2 system (a) and corresponding van't Hoff plots (b).

and La_2Co_7 (Gd_2Co_7 type; $R\bar{3}m$; a=5.13, c=36.66 Å) with weight ratio of phases equal to 52:23:25 and 42:14:44 for $LaMgCo_4$ and La_2MgCo_9 alloys, respectively. The availability of binary $RECo_2$/$RECo_3$ compounds in such systems seems to be a key factor for the formation of ternary or quasi-binary compounds. There are no such compounds in La–Co system, but, in the *RE*–Mg–Co systems (*RE*=Y, Pr, Nd) for which $RECo_2$/$RECo_3$ compounds are known, we have found ternary compounds. Results of studies of the last systems will be published elsewhere.

3.2. *Thermodynamic characteristics of $CeMgCo_4$–H_2 and Ce_2MgCo_9–H_2 systems*

The $CeMgCo_4$ compound at room temperature under pressures up to 100 bar H_2 easily absorbs hydrogen up to 6H/$CeMgCo_4$ content. It is worth to emphasize that under the same conditions isostructural Ni-based compound, $CeMgNi_4$, does not form any hydride.

PCT dependences for the $CeMgCo_4$–H_2 system are shown in Fig. 2, thermodynamic parameters of which are provided in Table 2. The absorption and desortpion occur with two plateaux corresponding to the following tranformations: α-$CeMgCo_4H_{\sim 0.2}$ ↔ β-$CeMgCo_4H_{\sim 4}$ and β-$CeMgCo_4H_{\sim 4}$ ↔ γ-$CeMgCo_4H_{\sim 6}$. The enthalpy and entropy of α ↔ β and β ↔ γ transitions have been calculated proceeding from middle-plateau points on absorption and desorption curves (Fig. 2b). At 20 °C under 10 bar H_2 hydrogen content in material is close to 4.2 H/$CeMgCo_4$, which value is still below the start of the β → γ transition. These results well agree with results of neutron diffraction analysis of the $CeMgCo_4D_{4.2}$ deuteride described below.

When comparing hydrogenation properties of $CeMgCo_4$ and $CeCo_2$ compounds it should be noted that the former has substantially lower hydrogenation capacity (1H/M compared with 1.33H/M). On the other hand it is much more stable against hydrogen induced amorphisation and disproportionation, whereas $CeCo_2$ irreversibly amorphise even under 40 bar H_2 at 50 °C [23].

Absorption and desorption isotherms and corresponding van't Hoff's plots for the Ce_2MgCo_9–H_2 system are shown in Fig. 3. Calculated values of enthalpy and entropy are provided in Table 2. The two-phase plateau, corresponding to equilibrium between α-$Ce_2MgCo_9H_{\sim 0.8}$ and β-$Ce_2MgCo_9H_{\sim 10.5}$ is rather horizontal, hysteresis between absorption and desorption is P_{ABS}/P_{DES}=5. Maximum observed capacity at 20 °C is 11.3H/Ce_2MgCo_9 reached at 50 bar H_2.

As follows from comparison of thermodynamic properties for Ce_2MgCo_9–H_2 and $CeCo_3$–H_2 systems [24], the partial Mg substitution for Ce in $CeCo_3$, accompanied by slight contraction of the unit cell, leads to substantial decrease in stability of the material (ΔH_{des}=27.2 compared to 38.1 kJ/mol H_2 [24]), with increase of plateau pressures by two orders of magnitude. In the $CeCo_3$–H_2 system a two-plateau desorption behavior has been observed, corresponding to formation of $CeCo_3H_3$ and $CeCo_3H_4$ hydrides

Table 2
Thermodynamic characteristics of PCT equilibria in the $CeMgCo_4$–H_2 and Ce_2MgCo_9–H_2 systems.

	$CeMgCo_4$–H_2				Ce_2MgCo_9–H_2	
	α↔β		β↔γ		α↔β	
	ΔH (kJ/mol)	ΔS (J/mol K)	ΔH (kJ/mol)	ΔS (J/mol K)	ΔH (kJ/mol)	ΔS (J/mol K)
Desorption	37 ± 1	121 ± 3	35.3 ± 0.9	125 ± 3	-27.2 ± 0.2	-120.9 ± 0.8
Absorption	-40.2 ± 0.8	-135 ± 2	-29.8 ± 0.2	-122.6 ± 0.8	-27.8 ± 0.5	-109.2 ± 1.7

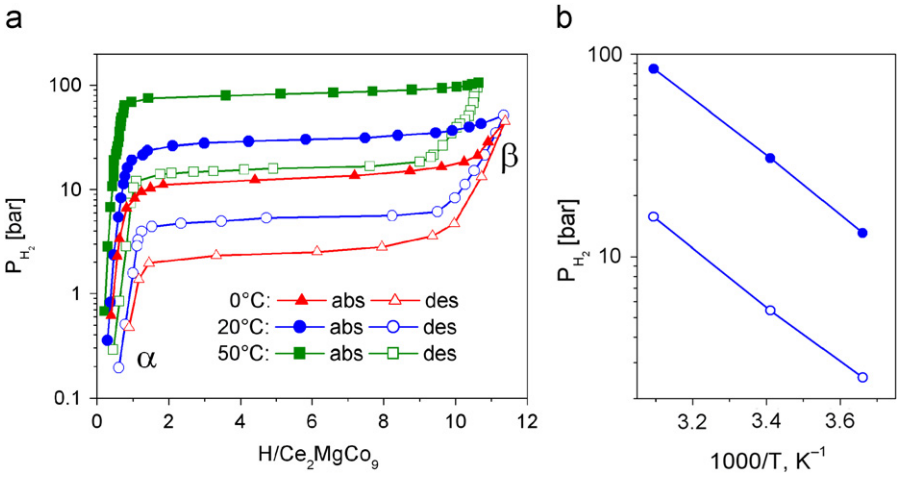

Fig. 3. Absorption and desorption isotherms for the Ce_2MgCo_9—H_2 system (a) and corresponding van't Hoff plots (b).

[24]. Introduction of magnesium into $CeCo_3$ decreases capacity from 1 to 0.95H/M, at the same time gravimetric H storage capacity is slightly increased from 1.26 to 1.35 wt% H due to substitution of Ce by much lighter element Mg.

3.3. Structure of hydrides of Ce–Mg–Co compounds

The prepared single-phase $CeMgCo_4$ alloy has been hydrogenated at 4 bar H_2, forming hydride with the $CeMgCo_4H_{\sim 4}$ composition. The unit cell expands by 20% (a=7.5050(3) Å; V=422.71(4) Å^3). The metal matrix of the compound preserves initial symmetry, showing no orthorhombic distortion as observed in structures of β-$LaMgNi_4D_{3.7}$ [8] and β-$NdMgNi_4D_{3.6}$ [16]. Atomic parameters of Co atoms (x=0.6257(7)) and distribution of Ce and Mg atoms between 4*a* and 4*c* sites remained almost unchanged as well.

PND patterns of the deuterated multiphase Ce–Mg–Co alloy with separated contributions from constituent phases are shown in Fig. 4. Results of full-profile Rietveld refinements of neutron diffraction data are provided in Table 3. In these refinements we have fixed distribution of Ce and Mg atoms between crystal sites, using the occupancy factors determined above from the XRD analysis instead, because the XRD pattern provide much stronger contrast between Ce and Mg than the PND experiment (b_{Ce}=4.84 fm; b_{Mg}=5.375 fm [21]). In good agreement with the above PCT measurements, the deuterated sample contained β-$CeMgCo_4D_{4.2}$ and α-$Ce_2MgCo_9D_{0.29}$ deuterides. In addition, the powder neutron diffraction revealed the presence of small amount, 0.4 wt.%, of magnesium oxide ($Fm\bar{3}m$; NaCl type; a=4.2162(6) Å), not detected in the XRD experiment. The unit cell volume of deuterated $Ce_{2.1}Mg_{1.9}Co_9$ was found to be noticeably larger than that of the initial non-deuterated phase, which fact clearly indicates the formation of solid solution of hydrogen in $Ce_{2.1}Mg_{0.9}Co_9$. On the basis of differential Fourier analysis in this structure small amounts of deuterium atoms have been

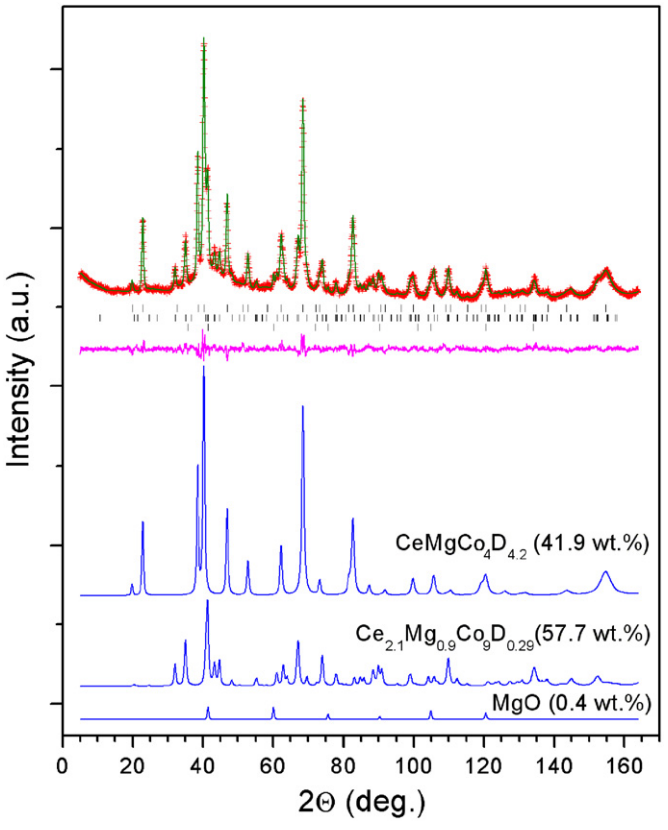

Fig. 4. Neutron powder diffraction patterns of the deuterated Ce–Mg–Co alloy, showing observed (+), calculated (upper line) and difference (lower line) profiles. Contribution from separate phases into overall diffraction patterns are shown below. Positions of Bragg's peaks are shown by bars in the same order as partial patterns.

localized in Co_3 face between two neighboring $CeCo_3$ tetrahedra and in $Ce(Mg/Ce)Co_2$ tetrahedra. The formation of α-$Ce_2MgCo_9D_{0.29}$ well agrees with PCT measurements, according to which saturated hydride of this compound is formed at room temperature in 25–45 bar H_2 pressure range (see Fig. 3).

The $CeMgCoD_{4.2}$ deuteride continues the series of structurally characterized deuterides of $RMgT_4$ compounds. There are earlier published results for β-$LaMgNi_4D_{3.7}$, γ-$LaMgNi_4D_{4.85}$ [8] and β-$NdMgNi_4D_{3.6}$ [16]. Crystallographic data of these deuterides and distribution of D-atoms among occupied interstices together with our findings are provided in Table 4. As can be seen from the table more than 70% of absorbed deuterium is accommodated in triangular MgT_2 faces common for two neighboring $RMgT_2$ tetrahedra. The deuteration of Ni-containing ternary compounds up to 3.5–4 at. D/f.u. causes orthorhombic distortion of the unit cell adopting $Pnm2_1$ space group. In the higher γ-$LaMgNi_4D_{4.85}$ distortion however disappears and $F\bar{4}3m$ space group recovers.

The lattice parameters of $CeMgCo_4D_{4.2}$ are rather close to those determined by SR XRD for the single-phase $CeMgCo_4H_{\sim 4}$. In the structure D atoms fill only one type of interstices—the $MgCo_2$ triangular faces, which form octahedra around magnesium atom with $d_{D-D}=2.595$ Å (Fig. 5). Octahedral coordination of magnesium by D atoms has been observed earlier in the structures of MgD_2 [25] (both α- and γ-polymorphs) and $La_{1.5}Mg_{0.5}Ni_7D_9$ [7]. Such coordination is also typical for magnesium based saline hydrides [26]. In addition to octahedra around Mg atoms D-sublattice in the structure of $CeMgCo_4D_{4.2}$ contains a little larger regular octahedra ($d_{D-D}=2.712$ Å) around the 4*d* site (3/4 3/4 3/4). This point is the center of the Co_4 tetrahedron, so six D atoms appear to be situated over Co–Co edges (Fig. 6a). It should be noted that a cluster around empty Ni_4 tetrahedra has been analyzed as well in structures of β-$LaMgNi_4D_{3.7}$ [8] and β-$NdMgNi_4D_{3.6}$ [16]. In these structures the cluster contains only four D-atoms, one of which caps the Ni_3 face being positioned in $RENi_3$ tetrahedron (see Fig. 6b). In addition to MgT_2 faces occupied in $CeMgCo_4D_{4.2}$ the structure of γ-$LaMgNi_4D_{4.85}$ has partially occupied Ni_4 tetrahedra (4*b*) [8]. The corresponding 4*b* Co_4 tetrahedra in the structure of $CeMgCo_4D_{4.2}$ remain empty. This site is the only position distance from which to the available D atoms exceeds 2.0 Å, a lower limit for D–D distances in interstitial hydrides.

Table 3
PND refinement results of deuterated Ce–Mg–Co alloy.

Atom	Site	*x*	*y*	*z*	$U_i/U_e \times 100$	Fractn
$CeMgCo_4D_{4.21(3)}$; *F*3–4*m*; *a*=7.5063(3) Å; *V*=422.94(3) Å^3						
Ce	4*a*	0	0	0	4.3(2)	0.94(–)
Mg1	4*a*	0	0	0	4.3(2)	0.06(–)
Mg	4*c*	1/4	1/4	1/4	4.9(1)	0.94(–)
Ce2	4*c*	1/4	1/4	1/4	4.9(1)	0.06(–)
Co	16*e*	0.6257(4)	*x*	*x*	1.31(6)	1.00(–)
D1	24*g*	0.0055(4)	1/4	1/4	3.33(5)	0.702(5)
$Ce_{2.1}Mg_{0.9}Co_9D_{0.29(6)}$; *R*–3*m*; *a*=4.9615(3); *c*=24.283(3) Å; *V*=517.69(9) Å^3						
Ce1	3*a*	0	0	0	2.5(2)	1.00(–)
Ce2	6*c*	0	0	0.1382(2)	3.1(1)	0.55(–)
Mg2	6*c*	0	0	0.1382(2)	3.1(1)	0.45(–)
Co1	3*b*	0	0	1/2	4.1(4)	1.00(–)
Co2	6*c*	0	0	0.3369(4)	2.5(3)	1.00(–)
Co3	18*h*	0.5033(7)	0.4967(7)	0.0849(2)	0.10(5)	1.00(–)
D1	18*h*	0.504(2)	0.496(2)	0.0214(6)	2.00	0.019(5)
D2	18*h*	0.122(7)	0.878(7)	0.930(3)	2.00	0.030(5)

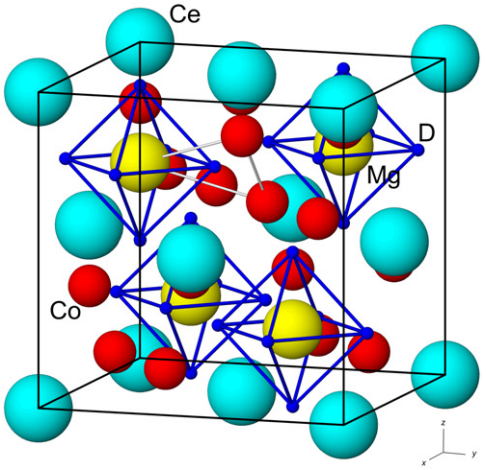

Fig. 5. Crystal structure of the $CeMgCo_4D_{4.2}$ deuteride. Octahedra of *D*-sites around Mg atoms are shown. One of occupied $MgCo_2$ faces is outlined.

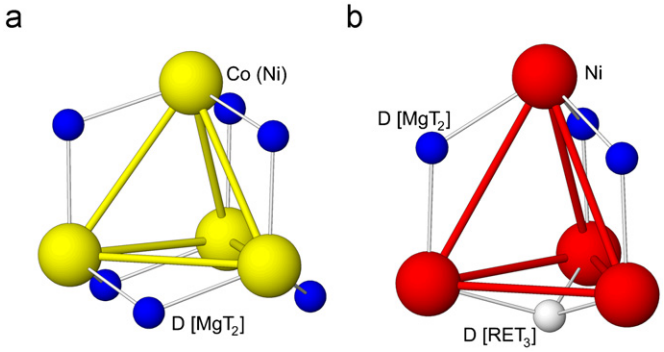

Fig. 6. Fragments of crystal structure of $REMgT_4D_x$ compounds: $Co(Ni)_4D_6$ clusters in $CeMgCo_4D_{4.21}$ and γ-$LaMgNi_4D_{4.85}$ (a) and Ni_4D_4 cluster in β-$La(Nd)MgNi_4D_{3.6}$ built on the data from [16](b).

Table 4
Distribution of D atoms and interatomic distances in occupied triangular MgT_2 faces (*T*=Co, Ni) in hydrides of $REMgT_4$ compounds (*RE*=La, Nd, Ce).

IMC	$LaMgNi_4$ [8]		$NdMgNi_4$ [16]	$CeMgCo_4$
at. H/f.u.	3.7	4.85	3.6	4.21
Space group	$Pnm2_1$	$F\bar{4}3m$	$Pnm2_1$	$F\bar{4}3m$
Lattice parameters (Å)	*a*=5.12570, *b*=5.52436, *c*=7.45487	*a*=7.65840	*a*=5.0767, *b*=5.4743, *c*=7.3792	*a*=7.5063
Occupied interstices (at. H/f.u.)				
MgT_2	2.68	4.32	2.733	4.21
$RENi_3$	1.0	–	0.899	–
Ni_4	–	0.54	–	–
Interatomic distances (Å)				
D–Mg	2.138–2.221	2.010	2.173–2.205	1.835
D–*T* (*T*=Ni, Co)	1.643–1.703	1.634	1.641–1.722	1.646

The refined deuterium content in $CeMgCo_4D_{4.2}$ is close to the determined by volumetric measurements and corresponds to the point on the PCT diagram between two plateaus of absorption/desorption. The capacity of 70% can be realized when four octahedron vertices are filled. However such a filling revealed no ordering of hydrogen sublattice, since no peaks on the PND pattern not allowed by $F\bar{4}3m$ space group have been observed. As can be seen from the Fig. 2a, further increase in H_2 pressure above 30 bar would allow synthesize deuteride with higher capacity, reaching 6H/$CeMgNi_4$ as maximum. Such capacity is reached, perhaps, when all six vertices of the MgH_6 octahedron are occupied. The transition from tetrahydride to hexahydride can proceed by two scenarios—as a continuous solid solution of hydrogen in $CeMgCo_4D_4$, or as a two-phase transition. As follows from the PCT results, the latter scenario seems more reasonable, since we observed the upper plateau. The study of structures of $CeMgCo_4D_6$ and $Ce_2MgCo_9D_{\sim 10}$ with the use of high-pressure in situ setup for PND measurements is planned for the future.

It should be emphasized that the occupied triangular $MgCo_2$ face in $CeMgCo_4D_{4.2}$ is characterized by unexpectedly short Mg–D distance of 1.835 Å, although D–Co distances remain in the same range as D–Ni ones in other studied deuterides (see Table 4). In binary MgD_2 the Mg–D distances, 1.915–2.004 Å [25], are noticeably larger than that in the $CeMgCo_4D_{4.2}$.

It is the shortest distance among known deuterides of Mg-containing intermetallic compounds. On the other hand existence of even shorter Mg–D separation, 1.77 Å, observed in $EuMg_2D_6$ have been attributed to partially covalent character of magnesium–deuterium (hydrogen) bonds [26].

4. Conclusions

Two new ternary compounds have been synthesized in the Ce–Mg–Co system: Ce_2MgCo_9 and $CeMgCo_4$. The former can be considered as a substitution derivative of $CeCo_3$ ($PuNi_3$-type structure) with Mg partially replacing Ce exclusively in the 6*c* site, the latter is isostructural to earlier studied *R*$MgNi_4$ compounds, but is the first the Co-containing one. The Ce_2MgCo_9 compound, similar to $La_{3-x}Mg_xNi_9$ (x=0.5–2) [7] has a homogeneity region in the *RE*/Mg content. The stoichiometric $CeMgCo_4$ is characterized by partial Ce/Mg disorder between 4*a* and 4*c* sites, similar to that found in $CeMgNi_4$ [15].

The new compounds absorb hydrogen at room temperature and pressures below 100 bar forming hydrides with maximum compositions $CeMgCo_4H_6$ and $Ce_2MgCo_9H_{12}$. The PCT study of hydrogenation properties of these compounds revealed that introduction of magnesium, accompanied by shrinking of the unit cell, decreases thermodynamic stability of their hydrides as compared to those of $CeCo_2$ and $CeCo_3$, respectively. Magnesium causes as well slight decrease in H/M capacity. The $CeMgCo_4$–H_2 system is characterized by the presence of two absorption/desorption plateau associated with formation of β-$CeMgCo_4H_4$ and γ-$CeMgCo_4H_6$ hydrides. Analysis of SR XRD and PND data for the β-$CeMgCo_4D_{4.2}$ deuteride structure revealed that, in contrast to hydrides of isostructural *RE*$MgNi_4$, it does not undergo orthorhombic transformation around 4H/f.u. composition. In the structure a very short Mg–H distance, 1.84 Å, has been observed.

References

[1] M. Dornheim, S. Doppiu, G. Barkhordarian, U. Boesenberg, T. Klassen, O. Gutfleisch, R. Bormann, Scr. Mater. 56 (2007) 841–846.
[2] R.V. Denys, A.B. Riabov, J.P. Maehlen, M.V. Lototsky, J.K. Solberg, V.A. Yartys, Acta Mater. 57 (2009) 3989–4000.
[3] G. Lu, L. Chen, L. Wang, H. Yuan, J. Alloys Compd. 321 (2001) L1–L4.
[4] R.V. Denys, I. Yu Zavaliy, V. Paul-Boncour, V.V. Berezovets, I.V. Koval'chuk, A.B. Riabov, Intermetallics 18 (2010) 1579–1585.
[5] T. Kohno, H. Yoshida, F. Kawashima, T. Inaba, I. Sakai, M. Yamamoto, M. Kanda, J. Alloys Compd. 311 (2000) L5–L7.
[6] R.V. Denys, A.B. Riabov, V.A. Yartys, Masashi Sato, R.G. Delaplane, J. Solid State Chem. 181 (4) (2008) 812–821.
[7] R.V. Denys, V.A. Yartys, J. Alloys Compd. 509 (Suppl. 2) (2011) S540–S548.
[8] J.-N. Chotard, D. Sheptyakov, K. Yvon, Z. Kristallogr. 223 (2008) 690–696.
[9] H. Oesterreicher, H. Bittner, J. Less-Common Met. 73 (1980) 339–344.
[10] C. Geibel, U. Klinger, M. Weiden, B. Buschinger, F. Steglich, Physica B 237–238 (1997) 202–204.
[11] K. Kadir, D. Noréus, I. Yamashita, J. Alloys Compd. 345 (2002) 140–143.
[12] S. Linsinger, M. Eul, Ch. Schwickert, R. Decourt, B. Chevalier, U.Ch. Rodewald, J.-L. Bobet, R. Pöttgen, Intermetallics 19 (10) (2011) 1579–1585.
[13] J.-G. Roquefere, B. Chevalier, R. Pöttgen, N. Terashita, K. Asano, E. Akiba, J.-L. Bobet, Intermetallics 16 (2008) 179–187.
[14] K. Aono, S. Orimo, H. Fujii, J. Alloys Compd. 309 (2000) L1–L4.
[15] J.-G. Roquefere, S.F. Matar, J. Huot, J.-L. Bobet, Solid State Sci. 11 (2009) 1971–1978.
[16] L. Guénée, V. Favre-Nicolin, K. Yvon, J. Alloys Compd. 348 (2003) 129–137.
[17] N. Hanada, S. Orimo, H. Fujii, J. Alloys Compd. 356–357 (2003) 429–432.
[18] Z.M. Wang, H.Y. Zhou, G. Cheng, Z.F. Gu, A.B. Yu, J. Alloy Compd. 384 (2004) 279–282.
[19] M. Knapp, C. Baehtz, H. Ehrenberg, H. Fuess, J. Synchrotron Rad. 11 (2004) 328–334.
[20] P. Fischer, G. Frey, M. Koch, M. Könnecke, V. Pomjakushin, J. Schefer, R. Thut, N. Schlumpf, R. Bürge, U. Greuter, S. Bondt, E. Berruyer, Physica B 276–278 (2000) 146–147.
[21] J. Rodriguez-Carvajal, Commission on Powder Diffraction (IUCr). Newsletter 26 (2001) 12–19.
[22] C.H. Wu, Y.C. Chuang, X.M. Jin, X.H. Guan, Z. Metallknd. 82 (1991) 621R–625R.
[23] R.H. van Essen, K.H.J. Buschow, J. Less-Common Met. 70 (1980) 189–198.
[24] V.V. Burnasheva, V.V. Klimeshin, K.N. Semenenko, Inorg. Mater. (Rus.) 15 (1979) 251–255.
[25] M. Bortz, B. Bertheville, G. Böttger, K. Yvon, J. Alloys Compd. 287 (1999) L4–L6.
[26] K. Yvon, B. Bertheville, J. Alloys Compd. 425 (2006) 101–108.